

# An integrated optimal control model for the drying and preheating process in iron ore pellet manufacturing

Ironmaking &amp; Steelmaking

2024, Vol. 51(1) 72–79

© The Author(s) 2024

Article reuse guidelines:

sagepub.com/journals-permissions

DOI: 10.1177/03019233231215182

journals.sagepub.com/home/ist



Xiaoxian Huang<sup>1</sup>, Xiaohui Fan<sup>1</sup>, Zongping Li<sup>2</sup>, Xuling Chen<sup>1</sup>,  
Zitang Peng<sup>1</sup>, Min Gan<sup>1</sup>, Zhiyun Ji<sup>1</sup> and Zengqing Sun<sup>1</sup>

## Abstract

The drying and preheating process plays a crucial role in the induration of iron ore pellets. It is conducted on a closed, moving bed in both the straight grate and grate-kiln processes. The internal state of the pellet bed cannot be measured and the manipulated parameters are set according to the experience. An integrated optimal control model based on the numerical simulation and intelligent algorithm is proposed. In this model, the moisture content and temperature of pellets in each stage are predicted via the mathematical simulation, and the inlet gas temperature is optimally set and real-time controlled through the multi-objective optimisation and Takagi–Sugeno fuzzy control methods. The proposed model has been successfully applied to a large-scale pelletising plant. The closed-loop running results illustrate that the thermal state of the pellet bed becomes stable, and the pellet production is improved while the mixed gas consumption is reduced.

## Keywords

iron ore pelletising, drying and preheating, numerical simulation, intelligent control

Received: 8 July 2023; accepted: 2 November 2023

## Introduction

Sintering and pelletising are the two most commonly used iron ore treatment processes. These processes involve transforming iron ore fines into bulk materials for ironmaking through high-temperature induration. While sintering is a popular choice, the pelletising process has lower energy consumption and pollutant emissions, and its product can be used as raw materials for both blast furnace and direct reduction processes. But pellets only make up 20% of the blast furnace burden structure in China,<sup>1</sup> leaving plenty of room for growth in pellet production. Improving the intelligent and green level of pelletising production can play a positive role in promoting pelletising technology and increasing pellet output.

During the drying and preheating (PH) process, the green pellet bed undergoes a complex exchange of heat with high-temperature air, leading to a series of chemical reactions such as water evaporation, magnetite oxidation, and carbonate decomposition.<sup>2</sup> However, due to the closed system of production equipment and the intricate nature of the reaction process, many state parameters cannot be directly measured. As early as the 1980s, Young et al.,<sup>3</sup> Thurlby et al.<sup>4</sup> and Thurlby<sup>5</sup> established some relatively complete simulation models for travelling grate and moving grate-rotary kiln, which laid the foundation for subsequent research. These

models accurately captured the main reaction processes, including water evaporation and condensation, magnetite oxidation and coke powder combustion. Barati<sup>6</sup> established a simulation model for the pelletising process in the travelling grate, which accounted for the shrinkage of pellets and the resulting drop in the pellet bed. Ljung et al.<sup>7</sup> developed a two-dimensional discrete model that combined with a continuous one-dimensional model to study the heat and mass transfer in the drying stage of the pellet bed. Fan et al.<sup>8,9</sup> went even further by building process simulation models of moving grates, rotary kilns, and ring coolers based on the principles of heat and mass transfer and physical–chemical reaction kinetics. By coupling these three models in an innovative way, they were able to make online predictions of the internal temperature field and reaction progress.

<sup>1</sup>School of Minerals Processing and Bioengineering, Central South University, Changsha, Hunan, PR China

<sup>2</sup>Zhongye Changtian International Engineering Co., Ltd, Changsha, Hunan, PR China

### Corresponding author:

Xiaoxian Huang, School of Minerals Processing & Bioengineering, Central South University, No. 932, South Lushan Road, Changsha, Hunan 410083, PR China.

Email: huangxiaoxian@csu.edu.cn



simulation results. Finally, the automatic control model adjusts manipulated variables such as fuel gas flow and fan gas flow in conjunction with the optimal setting values and inlet/outlet gas flow changes of each section. The integrated model provides a solution to the problems of soft measurement of state parameters, optimised setting of process parameters and intelligent control of operating parameters, which greatly improves the self-adaptive ability of the model and can be applied in the production field.

## Modelling

### Numerical simulation

The drying and PH process of pellets is a complex and non-linear phenomenon that exhibits significant hysteresis. The outlet gas temperature varies unpredictably when the inlet gas temperature changes in different sections, and this is influenced by a variety of factors such as the moisture content of the pellets and the thickness of the bed. The changes in pellet temperature, on the other hand, are slow to manifest and can take up to 30 min to become apparent. As a result, it is crucial to predict the outlet gas temperature in each section and the final pellet temperature during the optimisation process.

**Table 1.** Optimisation results of inlet gas temperature.

Items	Inlet gas temperature (°C)			
	UDD	DDD	TPH	PH
Original	231	375	741	1084
Optimised	201	359	755	1081

UDD: upward-draught drying; DDD: downward-draught drying; TPH: transition preheating; PH: preheating.

**Table 2.** The comparison of the thermal state.

Items	Outlet gas temperature (°C)					
	UDD	DDD	TPH	PH	$T_p$ (°C)	$f_e$ (%)
Original	94	144	273	411	1009	53.11
Optimised	88	131	247	390	998	59.25

UDD: upward-draught drying; DDD: downward-draught drying; TPH: transition preheating; PH: preheating.

**Table 3.** Training results of T-S fuzzy models.

Items		Model <sub>UDD</sub>	Model <sub>TPH</sub>	Model <sub>PH</sub>
Training set	$R^2$	0.800	0.878	0.938
	RMSE	15.49	41.86	36.12
Predicting set	$R^2$	0.825	0.903	0.958
	RMSE	17.75	45.57	67.96

T-S: Takagi-Sugeno; RMSE: root mean square error; UDD: upward-draught drying; PH: preheating; TPH: transition preheating.

In this study, a numerical simulation model is used to calculate the outlet gas temperature and the pellet temperature at the discharge end, considering the actual production conditions and the optimisation simulation with respect to the inlet gas temperature. The simulation model treats the bed layer as a one-dimensional convection-diffusion system along the gas flow direction. By dividing it into several units, the control equations of the system can be described based on the internal energy conservation and the component conservation of the gas-solid phase.

$$\begin{cases} GC_g \frac{\partial T_g}{\partial y} = -h_{\text{conv,eff}} A_{\text{ssa}} (T_g - T_p) + \sum_{i=1}^6 (1 - \lambda_i) R_i \Delta H_i \\ \rho_s C_p \frac{\partial T_p}{\partial t} = h_{\text{conv,eff}} A_{\text{ssa}} (T_g - T_p) + \sum_{i=1}^6 \lambda_i R_i \Delta H_i \\ -\frac{\partial P}{\partial y} = k_{a1} \cdot \frac{(1 - \varepsilon)^2 \mu_g v_g}{d_p^2 \varepsilon^3 \phi} + k_{a2} \cdot \frac{\rho_g (1 - \varepsilon) v_g^2}{d_p \varepsilon^3 \phi} \end{cases} \quad (1)$$

The simulation model considers the drying and condensation of moisture within the bed layer, removal of crystalline water, oxidation of magnetite, and decomposition of carbonate. The kinetic models for each reaction are represented by equations (2) to (6):

$$R_w = K_w A (W_g^e - W_g) \quad (2)$$

$$R_w = \frac{A(W_g^e - W_g)}{\left(\frac{1}{k_w}\right) + \left[\frac{r_p(r_p - r_w)}{2r_w D_{H_2O}^e}\right]} \quad (3)$$

$$R_{\text{geo}} = 50,700 \cdot \exp\left(-\frac{12,000}{T_p}\right) \cdot w_{\text{geo}} \quad (4)$$

$$R_m = \frac{29A(C_{O_2} - C_{O_2}^e)}{\left(\frac{1}{K_{O_2}}\right) + \left(\frac{r_p^2}{r_m^2}\right)\left(\frac{1}{k_m}\right) + \left(\frac{r_p}{D_{O_2}}\right)\left[\left(\frac{r_p}{r_m}\right) - 1\right]} \quad (5)$$

$$\begin{cases} R_L = \frac{44[4\pi \cdot r_l^2 n_l K_l (C_{CO_2}^e - C_{CO_2})]}{K_1 + K_2 + K_3} \\ K_1 = d_p(d_p - d_l) / d_l \cdot D_{CO_2}^e \\ K_2 = d_p / Sh \cdot D_{CO_2} \\ K_3 = 1 / [51,920 \cdot \exp(-22,251 / T_p)] \end{cases} \quad (6)$$

### Multi-objective optimisation

The objective of the pellet drying and PH procedure is to extract moisture from the pellets without any decrepitation. Simultaneously,  $Fe_3O_4$  is transformed into  $Fe_2O_3$ , and preheated pellets with a specific strength are produced. Throughout this operation, it is important to exploit the residual heat generated during roasting and cooling and to supplement the necessary heat with an external source. To refine the model and attain superior heat utilisation and decreased energy consumption, while guaranteeing the

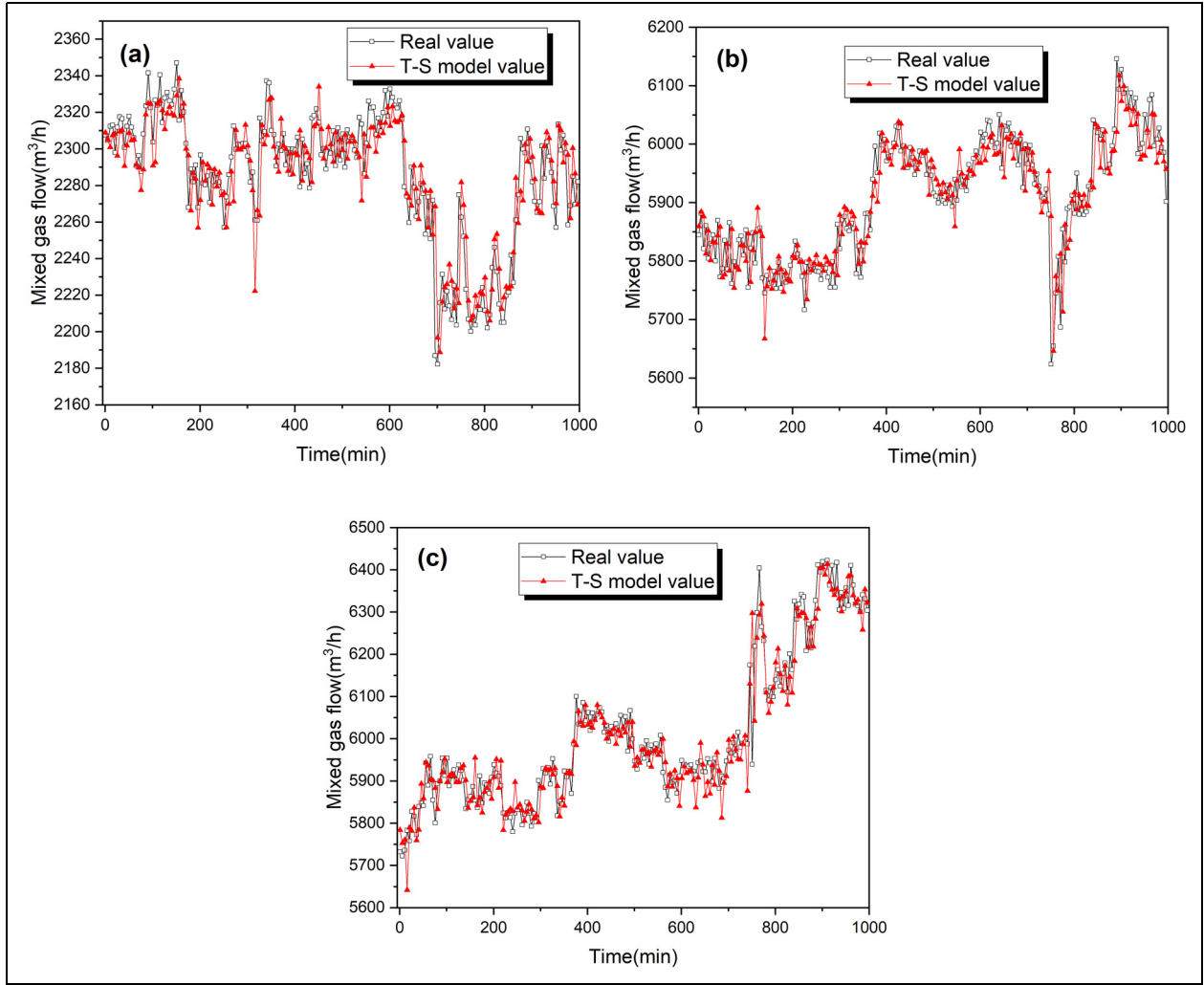


**Figure 2.** Mixed gas flow control results: (a) UDD section; (b) TPH section; and (c) PH section. UDD: upward-draught drying; PH: preheating; TPH: mild PH.

efficacy of pellet drying and PH. The optimisation model can be portrayed as equation (7):

$$\begin{aligned} \min f_e(x) &= H_p(x) / H_{in}(x) \\ \text{s.t. } \begin{cases} g_{pl}(x) \in [T_{p,\min}, T_{p,\max}] \\ g_{ogt}(x) \in [T_{OG,\min}, T_{OG,\max}] \end{cases} \end{aligned} \quad (7)$$

The search for maximum thermal efficiency in the pellet drying and PH process is a nonlinear optimisation problem that requires sophisticated techniques to solve. Among the methods commonly used are genetic algorithms, particle swarm algorithms, and other swarm intelligence algorithms. Genetic algorithms, for instance, are a randomised search technique that mimics the natural selection and genetic mechanisms in the biological world. They are ideal for optimising complex systems and possess robustness and global search capabilities, making them a popular choice in industrial production.<sup>19,20</sup> In this study, a real-valued encoded genetic algorithm is used to optimise the thermal efficiency of the pellet drying and PH process.

The algorithm follows the following steps:

- Step 1.** Randomly generate a set of inlet gas temperature configuration schemes.
- Step 2.** Utilise the numerical simulation model to calculate the thermal state of the pellet drying and PH process for each configuration scheme. This includes the pellet temperature at the discharge end and the gas temperatures at various outlets.
- Step 3.** Calculate the fitness of each scheme based on equation (1) and sort the schemes accordingly.
- Step 4.** Generate a new set of temperature configuration schemes through selection, crossover, and mutation operators.
- Step 5.** Check if the maximum evolution generation has been reached. If not, go back to Step 2. Otherwise, output the configuration scheme with the highest thermal efficiency.

### *T-S fuzzy control*

The intelligent control model for the pellet drying and PH process calculates the gas flow rates of the external heat sources in each section based on the optimised thermal

efficiency results. This ensures that the inlet gas temperature reaches the optimum value. In addition, real-time operating conditions are considered to make necessary adjustments to the inlet gas temperature set point. Therefore, the optimisation control of the inlet gas temperatures in each section cannot be implemented directly by a programmable logic controller. Instead, it requires the use of intelligent algorithms to mine production data and establish a secondary control model.

Expert systems, fuzzy logic control, and predictive control are commonly used modelling techniques in this context. Fuzzy control, in particular, has found wide application in industrial process control and robotics.<sup>21,22</sup> It exhibits robustness and high control performance when dealing with nonlinear and complex systems. The T-S fuzzy control model is a fuzzy logic system that represents rule consequences as functions of input variables. In this study, a T-S fuzzy model is used to establish the nonlinear relationship between the thermal state parameters of each section in the pellet drying and PH process and the gas flow rates of the heating sources.

For the heat supply of the pellet drying and PH process, the UDD section relies mainly on the hot flue gas from the third section of the grate cooler. However, if the flue gas temperature is insufficient, it can be heated by a hot air stove. In the DDD section, the primary source of heat comes from the PH section through hot flue gas. On the other hand, the TPH section is supplied mainly with hot flue gas from the second section of the cooler. If the flue gas temperature is low, it can be heated by a hot air stove or by igniting the burners on both sides of the hood.

PH section primarily is fed by the hot off-gas from the rear end of the rotary kiln and is supplied with heat from the combustion of the burners on either side of the hood.

Regarding the heat regulation in the pellet drying and PH process, the UDD and TPH sections are relatively independent, while the DDD and PH sections are coupled. In this study, separate T-S fuzzy control models are established for the UDD, TPH, and PH sections.

1. The UDD section's fuzzy control model is fuelled by a set of input parameters, including the deviation and deviation variation of the inlet and outlet gas temperatures. The output parameter is the mixed gas flow rate of the hot air stove.
2. The TPH section's fuzzy control model has similar input and output parameters as the UDD section's model. However, the output parameter can be converted into the mixed gas flow rate of the side burners.
3. The PH section adopts a fuzzy control model that considers a range of input parameters, including the deviation and deviation variation of the inlet and outlet gas temperatures, as well as the deviation and deviation variation of the outlet gas temperature in the DDD section. The model's output parameter is the gas flow rate of the hood-side burners.

All three fuzzy control models above are in the form of multiple inputs and single outputs, the process of building the T-S fuzzy control model of multiple-input single-output type is as follows: for the input variable  $x = [x_1, x_2, \dots, x_n]^T$ , the  $i$ th fuzzy rule can be expressed

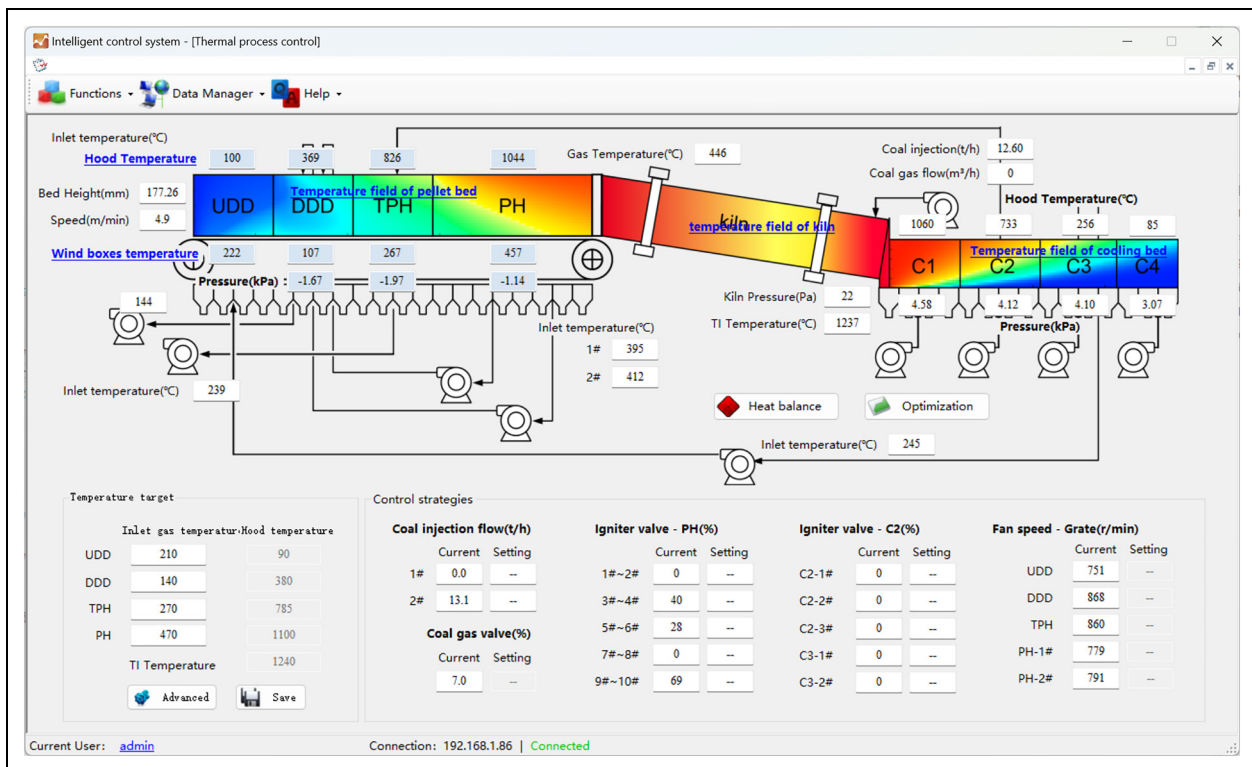
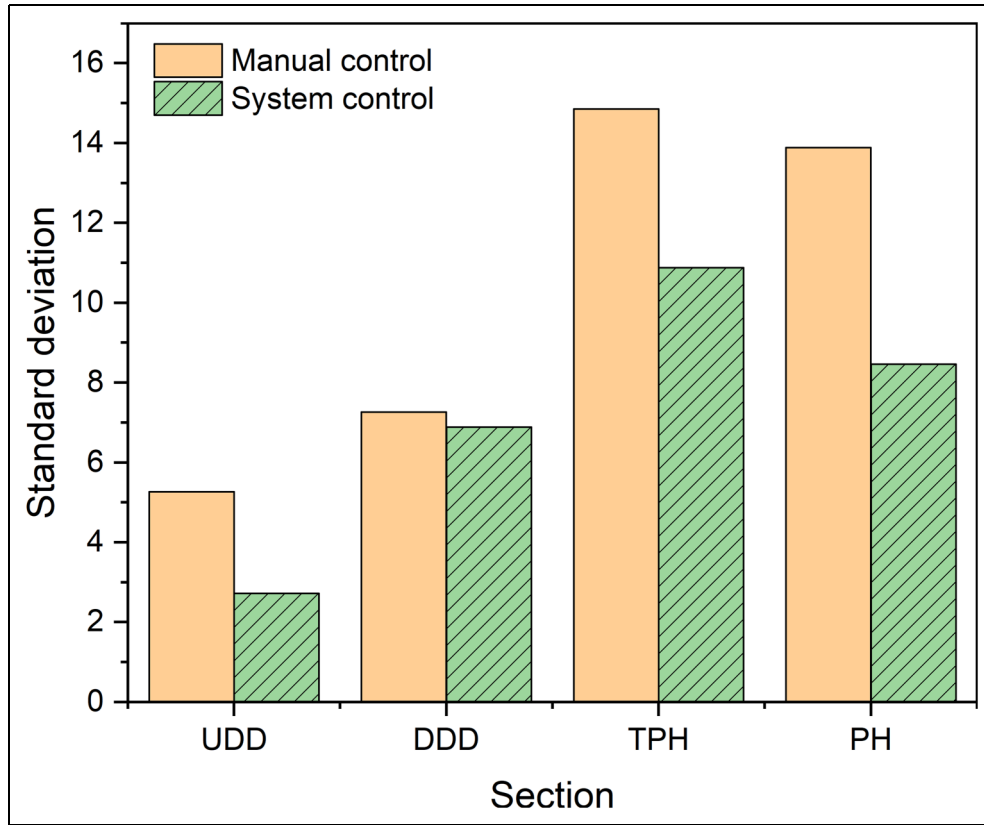


Figure 3. System interaction interface.



**Figure 4.** Comparison of temperature stability.

**Table 4.** The comparison of output, quality and energy consumption.

	Productivity (%)	Compressive strength (N/pellet)	Mixed gas consumption (m <sup>3</sup> /t)
Manual	77.84	2996	25.55
System	78.46	2916	24.43

as equations (8) and (9):

$$R^i: \text{If } x_1 \text{ is } U_{i1} \text{ and } x_2 \text{ is } U_{i2} \text{ and } \dots \text{ and } x_n \text{ is } U_{in} \quad (8)$$

$$\text{Then } y_i = w_i + w_{i1}x_1 + w_{i2}x_2 + \dots + w_{in}x_{2n}$$

$$U_i(x) = \prod_{j=1}^n U_{ij}(x_j) \quad (9)$$

The output of the fuzzy system is a weighted average of the output of each rule.

$$y = \frac{\sum_{i=1}^n \left( \frac{A_i(x)}{\sum_{i=1}^n A_i(x)} [1, x^T] w_i \right)}{\sum_{i=1}^n \left( \frac{A_i(x)}{\sum_{i=1}^n A_i(x)} \right)} \quad (10)$$

The creation of a T-S fuzzy model requires a clear understanding of the input variable's affiliation function and the rule posterior parameters. In this research, a unique approach combining subtractive clustering and fuzzy C-mean clustering is utilised to extract the fuzzy rules. The parameters of the rule posterior are then identified using the traditional least squares method.

## Case study and application

### Optimisation case

To validate the practicality of the thermal efficiency enhancement model, the initial conditions and boundary conditions of the simulation model were set based on actual working conditions. The pellet bed height was set at 200 mm, and the pellet's moisture content was 8 wt%. The proposed model optimised the inlet gas temperature of the drying PH process using a genetic algorithm with a population size of 20, a crossover probability of 0.5, a variation probability of 0.08, and an evolutionary generation of 200.

Table 1 illustrates the comparison of the inlet temperature before and after optimisation, revealing that the optimised UDD and DDD sections' inlet gas temperature decreased, while the TPH section increased, and the PH section remained relatively stable. The simulation model calculated the outlet gas temperature, pellet temperature ( $T_p$ ) at the discharge end, and thermal efficiency ( $f_e$ ) for the two operating parameters, as shown in Table 2. Under the optimised inlet gas temperature condition, the outlet gas temperature of each section decreased, and the PH pellet temperature at the discharge end difference was insignificant. The overall thermal efficiency of the drying PH process increased by approximately 12 wt%.

### Intelligent control case

The intelligent control model of the thermal state for the drying and PH process was trained by the production

field data. A total of 288 data sets, each taken at 5 min intervals over a 24 h period, were collected. Out of these, 200 sets were utilised for training purposes, while the remaining 88 sets were reserved for testing. The efficacy of the T–S fuzzy control model was evaluated for the UDD, TPH, and PH sections, as illustrated in Table 3. The correlation coefficient ( $R$ ) and root mean square error (RMSE) were the metrics used to gauge the accuracy of the model's predictions.

The UDD control model shows a surprising correlation coefficient in the prediction results. However, the RMSE is only  $17.75 \text{ m}^3/\text{h}$ , which is only 0.78% of the mean. The error range is also remarkably small. On the other hand, the TPH section and PH section control models both have correlation coefficients over 0.9. This indicates that the fitted values have a strong correlation with the actual values. Furthermore, their RMSEs are only 0.78% and 1.13% of the mean, respectively. These models have a high degree of predictive accuracy.

The trained model was further validated in the continuous production process, with Figure 2 displaying the predicted results of the control model for each 1000 min segment. The model's predictions for the mixed gas flow rate in each segment of this continuous production process were in remarkable agreement with the factual control value, signifying that the established control regulations could supplant the on-site operator in executing the closed-loop control of the thermal state of the drying PH process.

### Practical application

In this research, an advanced control system for the drying and PH process of a travelling grate-rotary kiln was developed upon the simulation-based optimisation model and intelligent control model. The system was developed using the C# programming language, and its interface is depicted in Figure 3. This innovative system was then implemented at a prominent pellet production site in China.

The standard deviation of the outlet gas temperature of the drying PH process before and after the system operation is illustrated in Figure 4, and the yield, quality and energy consumption indices of pellet ore are provided in Table 4.

The intelligent control system has successfully minimised the standard deviation of the outlet gas temperature in each section, resulting in a more reliable drying PH process. This has resulted in a remarkable 50% increase in the stability of the UDD section, which in turn ensures a consistent and safe heating process during drying, effectively preventing the thermal bursting of the pellets. In addition, the PH section has experienced a significant 40% increase in stability, which has facilitated the formation of robust  $\text{Fe}_2\text{O}_3$  crystal bonds within the pellets, thereby increasing their mechanical strength. This has also prevented the occurrence of internal cracking that may occur due to cooling after entering the kiln.

An examination of the data shows that meticulous optimisation controls have increased pellet output. Despite a slight reduction in the compressive strength of the final

pellets, it remains well above the production threshold of 2500 N. In addition, the utilisation of mixed gas per tonne of pellets has been significantly reduced.

### Conclusions

An integrated optimisation control approach and system for the drying and preheating process in pellet production are developed. The inlet gas temperature of each section is set by a thermal efficiency optimisation model, which is based on a mathematical model of the drying and preheating process. The recommended operation parameters can be calculated via an advanced control model, the mixed gas flow in each section was found to be in remarkable agreement with the actual control values in the field. An optimisation control system for the travelling grate-rotary kiln has been developed and successfully implemented at a large-scale pellet production site in China. The operation results indicated that the automatic control of the drying and preheating process resulted in a significant reduction in the standard deviation of the outlet gas temperature of each section. The stable control has resulted in a remarkable improvement in pellet yield while reducing the amount of mixed gas per tonne of finished pellets.

Work continues to further improve the generality and accuracy of the proposed approach, such as the different particle size distributions of pellets and the corresponding bed packing structures. Further, the optimisation model has to self-adaptively scale the parameter constraints according to the specific working conditions and to reinforce the stability of the solving process.

### Declaration of conflicting interests

The authors declared no potential conflicts of interest with respect to the research, authorship, and/or publication of this article.

### Funding

The authors disclosed receipt of the following financial support for the research, authorship, and/or publication of this article: This work was supported by the National Natural Science Foundation of China under Grant Nos. 51974371 and 51804347.

### References

1. Wang X. Design and production practice of blast furnace system for high proportion pellet smelting. *Iron Steel* 2022; 57: 23–31.
2. Copeland CR, Claremboux V and Kawatra SK. A comparison of pellet quality from straight-grate and grate-kiln furnaces. *Miner Process Extractive Metall Rev* 2019; 40: 218–223.
3. Young RW, Cross M and Gibson RD. Mathematical model of grate-kiln-cooler process used for induration of iron ore pellets. *Ironmaking Steelmaking* 1979; 6: 1–13.
4. Thurlby JA, Batterham RJ and Turner RE. Development and validation of a mathematical model for the moving grate induration of iron ore pellets. *Int J Miner Process* 1979; 6: 43–64.

5. Thurlby JA. Gas flow and pressure balancing in modeling grate/kiln induration. *Metall Mater Trans* 1988; 19: 113–121.
6. Barati M. Dynamic simulation of pellet induration process in straight-grate system. *Int J Miner Process* 2008; 89: 30–39.
7. Ljung A, Frishfelds V, Lundström TS, et al. Discrete and continuous modeling of heat and mass transport in drying of a bed of iron ore pellets. *Drying Technol* 2012; 30: 760–773.
8. Wang Y, Fan XH and Chen XL. Mathematical models and expert system for grate-kiln process of iron ore oxide pellet production (part I): mathematical models of grate process. *J Central South Univ* 2012; 19: 1092–1097.
9. Fan XH, Yang GM, Chen XL, et al. Predictive models and operation guidance system for iron ore pellet induration in traveling grate-rotary kiln process. *Comput Chem Eng* 2015; 79: 80–90.
10. Majumder S, Desai VJ, Arunprasath J, et al. Model-based on-line optimization of iron ore pellet induration on a moving grate furnace. In: 26th international mineral processing congress, IMPC 2012: Innovative processing for sustainable growth – conference proceedings, pp. 3117–3136.
11. Miriyala SS and Mitra K. Multi-objective optimization of iron ore induration process using optimal neural networks. *Mater Manuf Process* 2020; 35: 537–544.
12. Halt JA, Silva BB and Kawatra SK. A new on-line method for predicting iron ore pellet quality. *Miner Process Extract Metall Rev* 2015; 36: 377–384.
13. Yu H and Liu Q. Research on quality prediction of iron ore green pellets based on optimized neural network. In: 2022 3rd international conference on big data, artificial intelligence and internet of things engineering, ICBAIE 2022, pp. 377–382.
14. Dechevsky LT, Sziebig G and Korondi P. Optimizing the automation of an iron ore production line – a case study, part II: Optimal automated quality control. In: Proceedings – 2016 IEEE international power electronics and motion control conference, 2016, pp. 753–762.
15. Tan S, Peng J and Shi H. Modeling and simulation of iron ore pellet drying and induration process with accurate bed void fraction calculation. *Drying Technol* 2016; 34: 651–664.
16. Wang Y, Fan XH and Chen XL. Expert system for control guidance of grate-kiln pellet production. *ISIJ Int* 2013; 53: 399–402.
17. Yang G, Fan X, Chen X, et al. Intelligent control of grate-kiln-cooler process of iron ore pellets using a combination of expert system approach and Takagi-Sugeno fuzzy model. *J Iron Steel Res Int* 2016; 23: 434–441.
18. Wang Y, Fan X and Chen X. Mathematical models and expert system for grate-kiln process of iron ore oxide pellet production (Part I): mathematical models of grate process. *J Central South Univ Technol (Engl Ed)* 2012; 19: 1092–1097.
19. Mitra K and Majumder S. Successive approximate model based multi-objective optimization for an industrial straight grate iron ore induration process using evolutionary algorithm. *Chem Eng Sci* 2011; 66: 3471–3481.
20. Badrmezhad R and Mirza B. Modeling and optimization of cross-flow ultrafiltration using hybrid neural network-genetic algorithm approach. *J Ind Eng Chem* 2014; 20: 528–543.
21. Lohani A, Goel N and Bhatia K. Takagi-Sugeno fuzzy inference system for modeling stage-discharge relationship. *J Hydrol* 2006; 331: 146–160.
22. Yazdani-Chamzini A, Razani M, Yakhchali S, et al. Developing a fuzzy model based on subtractive clustering for road header performance prediction. *Autom Construct* 2013; 35: 111–120.

## List of symbols

### Notation

$A_{ssa}$	specific surface area ( $\text{m}^2 \text{m}^{-3}$ )
$C_p$	specific heat ( $\text{J kg}^{-1} \text{K}^{-1}$ )
$C$	molar concentration of gas phases ( $\text{mol m}^{-3}$ )
$d_p$	equivalent diameter of pellet (m)
$D$	mass diffusion coefficient of gas phases ( $\text{m}^2 \text{s}^{-1}$ )
$H$	height of sintering bed (m)
$\Delta H$	enthalpy of reaction ( $\text{J kg}^{-1}$ )
$H_p$	heat of the preheated pellets
$H_{in}$	total heat input
$h_{conv}$	convection heat transfer coefficient ( $\text{W m}^{-2} \text{K}^{-1}$ )
$eff$	
$k_{a1}$	viscous resistance coefficient
$k_{a2}$	inertial resistance coefficient
$k_c$	reaction rate constant of coke breeze combustion ( $\text{m s}^{-1}$ )
$K_{O_2}$	mass transfer coefficient of oxygen ( $\text{m s}^{-1}$ )
$M$	molecular weight ( $\text{kg mol}^{-1}$ )
$m_c$	un-reacted part mass ( $\text{kg m}^{-3}$ )
$m_0$	initial particle mass ( $\text{kg m}^{-3}$ )
$n_l$	number of carbonate particles per unit material
$P$	pressure (Pa)
$R$	reaction rate ( $\text{kg m}^{-3} \text{s}^{-1}$ )
$R_g$	universal gas constant ( $\text{J mol}^{-1} \text{K}^{-1}$ )
$r_m$	un-reacted core radius of magnetite (m)
$r_p$	radius of pellets (m)
$r_w$	wetting radius of pellets (m)
$r_0$	initial radius of limestone particle (m)
$r_c$	radius of limestone particle (m)
$Sh$	Sherwood number
$T$	temperature (K)
$U$	affiliation function of the input variable
$t$	time (s)
$v$	gas velocity ( $\text{m s}^{-1}$ )
$W_g$	moisture content ( $\text{kg m}^{-3}$ )
$w_i$	posterior parameter
$y$	pellet bed height (m)

### Greeks symbols

$\epsilon$	porosity of sinter bed or solid phases
$\rho$	density ( $\text{kg m}^{-3}$ )
$\lambda$	fraction of heat absorbed by solid
$\mu$	gas dynamic viscosity ( $\text{kg m}^{-1} \text{s}^{-1}$ )

### Subscripts and superscripts

g	gas phase
s	solid phase (pellets)
w	reaction of water evaporation and condensation
m	reaction of magnetite oxidation
l	reaction of carbonate decomposition
geo	reaction of crystalline water removal
e	equilibrium state